



## 强相互作用中的对称性破缺—手征磁效应

王福强

### Symmetry Breaking in the Strong Interaction – The Chiral Magnetic Effect

WANG Fuqiang

在线阅读 View online: <https://doi.org/10.11804/NuclPhysRev.41.2023CNPC55>

引用格式:

王福强. 强相互作用中的对称性破缺—手征磁效应[J]. *原子核物理评论*, 2024, 41(1):1–10. doi: 10.11804/NuclPhysRev.41.2023CNPC55

WANG Fuqiang. Symmetry Breaking in the Strong Interaction – The Chiral Magnetic Effect[J]. *Nuclear Physics Review*, 2024, 41(1):1–10. doi: 10.11804/NuclPhysRev.41.2023CNPC55

---

## 您可能感兴趣的其他文章

### Articles you may be interested in

#### 强相互作用系统的对称性及其破缺

Symmetries and Their Breaking of Strong Interaction System

原子核物理评论. 2020, 37(3): 329–363 <https://doi.org/10.11804/NuclPhysRev.37.2019CNPC77>

#### 强磁场与涡旋场中的夸克胶子物质

Quark Gluon Matter in Strong Magnetic and Vortical Fields

原子核物理评论. 2020, 37(3): 414–425 <https://doi.org/10.11804/NuclPhysRev.37.2019CNPC29>

#### 自旋与手征动力学的输运模拟研究

Studies on Spin and Chiral Dynamics with Transport Simulations

原子核物理评论. 2020, 37(3): 650–659 <https://doi.org/10.11804/NuclPhysRev.37.2019CNPC22>

#### 动量相关势对直接流和椭圆流的影响

The Influence of the Momentum Dependence Potential on the Directed Flow and Elliptic Flow

原子核物理评论. 2022, 39(1): 16–22 <https://doi.org/10.11804/NuclPhysRev.39.2021071>

#### 利用格点量子色动力学研究手征平滑过渡温度和手征相变温度

Chiral Crossover and Chiral Phase Transition Temperatures from Lattice QCD

原子核物理评论. 2020, 37(3): 674–678 <https://doi.org/10.11804/NuclPhysRev.37.2019CNPC65>

#### 低能强流混合离子束空间电荷补偿度研究

Space Charge Compensation Study of Low-energy High-intensity Mixed Ion Beams

原子核物理评论. 2023, 40(1): 45–50 <https://doi.org/10.11804/NuclPhysRev.40.2022032>

# Symmetry Breaking in the Strong Interaction – The Chiral Magnetic Effect

WANG Fuqiang

(School of Science, Huzhou University, Huzhou 313000, Zhejiang, China)

**Abstract:** The chiral magnetic effect (CME) refers to a charge separation along a strong magnetic field due to an imbalanced chirality of quarks from interactions with the vacuum topological gluon field. This chiral anomaly is a fundamental property of quantum chromodynamics (QCD) and, therefore, an observation of the CME would have far-reaching impact on our understanding of QCD and Nature. The measurements of the CME-sensitive azimuthal correlator  $\Delta\gamma$  observable in heavy-ion collisions are contaminated by a major background induced by elliptic flow anisotropy. Several novel approaches have been carried out, including a dedicated isobar collision program, to address this flow-induced background. Further background effects, arising from nonflow correlations, have been studied. While the isobar data are consistent with zero CME signal with an upper limit of 10% of the measured  $\Delta\gamma$ , the Au+Au mid-central data suggest a positive CME signal on the order of 10% of the measured  $\Delta\gamma$  with a significance of  $\sim 2$  standard deviations. Future increased statistics and improved detector capability should yield a firm conclusion on the existence (or the lack) of the CME in relativistic heavy-ion collisions.

**Key words:** chiral magnetic effect; charge separation;  $\Delta\gamma$  correlator; flow-induced background; nonflow

**CLC number:** O571.3    **Document code:** A    **DOI:** [10.11804/NuclPhysRev.41.2023CNPC55](https://doi.org/10.11804/NuclPhysRev.41.2023CNPC55)

## 0 Introduction

Symmetry is the most important concept in physics. Physical laws are symmetric; their solutions are, however, unnecessarily so. In fact, our universe, a solution to the physical laws, is maximally asymmetric. For example, photons, which mediate the electromagnetic force, are massless, and those gauge bosons mediating the weak force are massive; quarks are not massless but massive with three generations. These asymmetries are the result of spontaneous electroweak symmetry breaking due to the vacuum Higgs field. Another example, the approximate chiral symmetry is spontaneously broken because of existence of the vacuum chiral condensate; interactions with the condensate give constituent quarks the majority of their mass and thus of all visible matter in the universe. Similarly, the  $U_A(1)$  symmetry, pertinent to quark chirality, is spontaneously broken because of the axial anomaly of the vacuum gluon pseudoscalar, a superposition of quantum states of all possible Chern-Simons winding numbers or topological charges [Fig. 1(a)]. The numbers of left- and right-handed quarks are no longer individually conserved in local domains because of interactions with the topological gluon

field. This would lead to local parity (P) and charge-conjugate parity (CP) violations in the quantum chromodynamics (QCD) strong interaction, which may be connected to the matter-antimatter asymmetry of our present-day universe.

The Higgs particle has been directly observed<sup>[1]</sup>. The quark-antiquark condensate has not been directly observed<sup>[2]</sup>, neither has been the axial chiral anomaly or the corresponding axion particle<sup>[3]</sup>. The non-zero net chirality (handedness) can, however, have observable consequence under a strong external magnetic field<sup>[4-5]</sup>—same-handed quarks depart according to their electric-charge dependent magnetic moments, either along or opposite to the magnetic field direction, a phenomenon called the chiral magnetic effect (CME)<sup>[6]</sup> [Fig. 1(b)]. Relativistic heavy-ion collisions may offer an opportunity to observe it: a deconfined quark-gluon plasma (QGP) is created sufficiently hot<sup>[7-8]</sup> that domains of non-zero topological charges can form, and a strong magnetic field is produced by the passing spectator protons at finite impact parameter<sup>[9]</sup> [Fig. 2(a)]. An observation of the CME would have far-reaching impact on our understanding of QCD and Nature.

This contribution reviews the current status of the experimental search for the CME, starting with early meas-

**Received date:** 09 Aug. 2023;    **Revised date:** 10 Jan. 2024

**Foundation item:** National Natural Science Foundation of China (12035006, 12075085); Ministry of Science and Technology of China (2020YFE020200)

**Biography:** WANG Fuqiang(1967–), male (USA), Huzhou, Zhejiang, Ph.D, working on relativistic heavy-ion collisions; E-mail: [fqwang@zjhu.edu.cn](mailto:fqwang@zjhu.edu.cn)

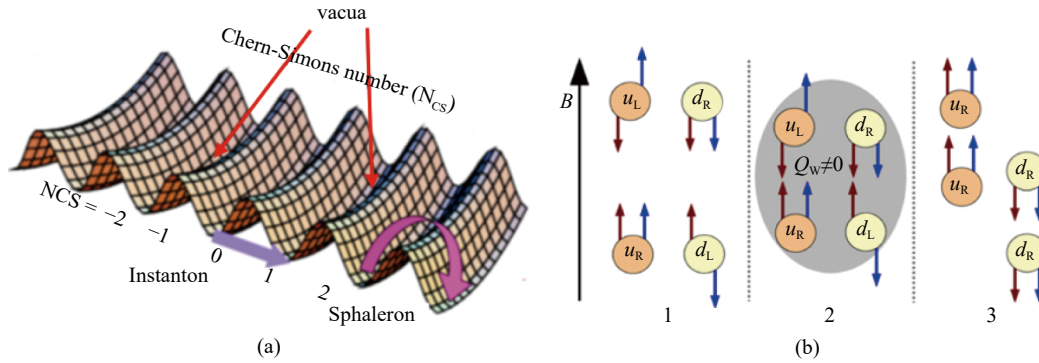


Fig. 1 (a) Sketch of the physical vacuum being superposition of states of all possible Chern-Simons winding numbers (topological charges). Sphaleron transitions between states may be appreciable at high temperatures. (b) Illustration of the CME<sup>[5]</sup>. The dark-brown arrows denote the direction of momentum, the blue arrows the spin of the quarks. 1) Initially there are as many left-handed as right-handed quarks. Due to the strong magnetic field the up and down quarks are all in the lowest Landau level and can only move along the magnetic field. 2) The quarks interact with a topological gluon field with non-zero topological charge ( $Q_w \neq 0$ ), converting left-handed quarks into right-handed ones (in this case  $Q_w < 0$ ) by reversing the direction of momentum. 3) The right-handed up quarks move upward, and the right-handed down quarks move downward, resulting in a charge separation. (color online)

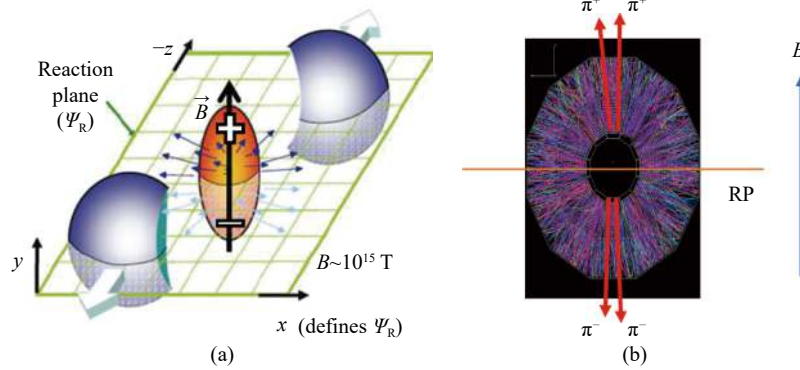


Fig. 2 (a) Schematic view of a non-central heavy-ion collision, where spectators pass each other proceeding in the beam direction, leaving participants in the overlap zone forming a QGP. The reaction plane (RP) is defined as the plane spanned by the beam and the impact parameter direction. A huge magnetic field, on the order of  $10^{15}$  Tesla at the first moment of encounter, is produced primarily by the passing spectator protons. (b) An event display of an Au+Au collision in the STAR Time Projection Chamber (TPC); the drawings depict the RP direction, the magnetic field direction that is on average perpendicular to the RP, and the back-to-back opposite-sign (OS) particle pairs from CME-induced charge separation and the same-sign (SS) pairs in the same direction parallel or antiparallel to the magnetic field. (color online)

measurements and a discussion on the major backgrounds, followed by recent measurements eliminating those backgrounds. It then continues with investigations of the next-level backgrounds, followed by remarks on possible remaining issues. Finally, a brief summary and outlook is given. The contribution is written in such a way that following the figures and captions should give the reader a fairly complete picture.

## 1 Observable, early measurements, and flow-induced backgrounds

A distinct signature of the CME is back-to-back emission of OS charged hadrons and collimated emission of SS ones in the direction of the magnetic field. Since the magnetic field created in non-central heavy-ion collisions is on average perpendicular to the RP, a commonly used observable<sup>[10]</sup> is the two-particle correlator

$$\gamma_{\alpha\beta} \equiv \langle \cos(\phi_\alpha + \phi_\beta - 2\psi_{RP}) \rangle, \quad (1)$$

where  $\phi_\alpha$  and  $\phi_\beta$  are the particle azimuthal angles with  $\alpha$  and  $\beta$  denoting their charge signs, and  $\psi_{RP}$  is the azimuthal angle of the RP. The CME signal would be  $\gamma_{OS} > 0$  and  $\gamma_{SS} < 0$ . Because of the existence of charge-independent background, the difference

$$\Delta\gamma_{\alpha\beta} \equiv \gamma_{OS} - \gamma_{SS} \quad (2)$$

is often used.

Figure 3 shows the first measurements of  $\gamma_{OS}$  and  $\gamma_{SS}$  at the Relativistic Heavy-Ion Collider (RHIC) by the STAR experiment<sup>[11–13]</sup> and at the Large Hadron Collider (LHC) by the ALICE experiment<sup>[14]</sup>. Large differences between  $\gamma_{OS}$  and  $\gamma_{SS}$  measurements were observed. The  $\Delta\gamma$  is on the order of  $10^{-4}$ , suggesting that  $\sim 1\%$  particles could be related to the CME if the measured  $\Delta\gamma$  magnitude is indeed all from CME.

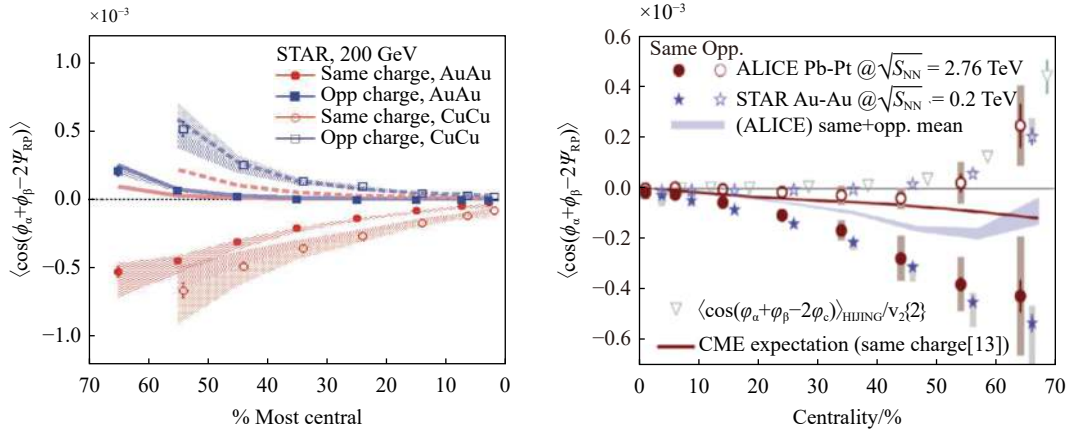


Fig. 3 First measurements of the  $\gamma$  correlators of OS and SS charged particle pairs in Au+Au and Cu+Cu collisions by RHIC/STAR<sup>[11–12]</sup> (a) and in Pb+Pb collisions by LHC/ALICE<sup>[14]</sup> (b) Large differences between the OS and SS correlators are observed, consistent with charge separation perpendicular to the reaction plane. Majority of the difference signal is due to flow-induced backgrounds, not of CME-induced charge separation. (color online)

Unfortunately, there remains charge-dependent backgrounds<sup>[10, 15–17]</sup>, e.g., those due to resonance decays and jet-like correlations. The  $\Delta\gamma$  is ambiguous between a back-to-back OS pair perpendicular to the RP (CME signal) and a collimated one parallel to it (background). Because of elliptic flow ( $v_2$ ), there are more resonances/clusters thus more OS pairs along the RP, leading to the background [Fig. 4(b)]. In other words, it arises from the coupling of  $v_2$  and genuine two-particle (2p) correlations<sup>[10, 18]</sup>,

$$\Delta\gamma_{\text{Bkg}} = \frac{N_{2p}}{N_\alpha N_\beta} \langle \cos(\phi_\alpha + \phi_\beta - 2\phi_{2p}) \rangle v_{2, 2p}, \quad (3)$$

where  $N$  stands for multiplicity and the subscript ‘2p’ stands for 2p-correlation sources. Order of magnitude estimate suggests a background level of  $0.2/100 \times 0.5 \times 0.1 \sim 10^{-4}$ , comparable to the measured  $\Delta\gamma$ . In fact, thermal and Blast-wave model parameterizations of particle yields and spectra data can reproduce the majority, if not the full, strength of the measurement<sup>[17, 19]</sup>. This is also corroborated by experimental data from small system collisions at both the LHC<sup>[20]</sup> and RHIC<sup>[21]</sup>. An explicit demonstration of resonance backgrounds is provided by the differential  $\Delta\gamma$  measurement as a function of the pair invariant mass<sup>[22]</sup>.

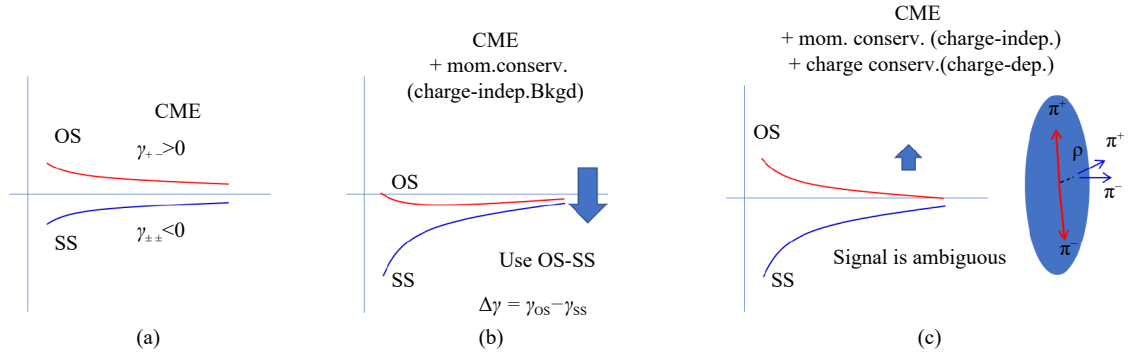


Fig. 4 Illustrations of CME signal and flow-induced backgrounds, depicted versus centrality in heavy-ion collisions. (a) The OS and SS  $\gamma$ -correlator signals are equal in magnitude and opposite in sign, and are diluted by event multiplicity because of the two-particle correlation nature of the  $\gamma$ -correlators. (b) Charge-independent backgrounds, such as those arising from momentum conservation preferring back-to-back emissions of particles, which are RP dependent due to elliptic flow anisotropy of particle azimuthal distributions, contribute a common negative signal to the OS and SS  $\gamma$ -correlators. These backgrounds are canceled in the  $\Delta\gamma = \gamma_{\text{OS}} - \gamma_{\text{SS}}$  observable. (c) Charge-dependent backgrounds, such as those from resonance decays coupled with resonance elliptic flow ( $v_{2,2p}$ ), contribute a positive signal to the OS  $\gamma$ -correlator and have a reduced/negligible contribution to the SS  $\gamma$ -correlator. These backgrounds can be expressed algebraically by Eq. (3). (color online)

## 2 Innovative ways to remove flow-induced backgrounds

Many innovative methods have been proposed to deal with the flow-induced backgrounds<sup>[18, 23]</sup>. Three most prominent ones are described below.

### 2.1 By varying background

One way to gain insight is to vary the background and see how  $\Delta\gamma$  responds to it. Since  $\Delta\gamma_{\text{Bkg}} \sim v_2$  [(Eq. (3))], one may vary  $v_2$  by the event shape engineering (ESE) technique<sup>[24–25]</sup>. This was first attempted by STAR<sup>[24]</sup> where the multiplicity asymmetry correlation (a quantity similar to

$\Delta\gamma$ ) is plotted against the observed ellipticity  $v_2^{\text{obs}}$  of particles of interest (POI) in one half of the STAR TPC with respect to the second-order event plane (EP, an experimental terminology referring to the harmonic symmetric plane<sup>[26]</sup>) reconstructed from the other half. A linear relationship is observed [Fig. 4(a)]. The  $v_2^{\text{obs}}$  can be negative because this ESE method engineers primarily on statistical fluctuations of  $v_2$ . The intercept at  $v_2^{\text{obs}}=0$  is more sensitive to the CME than the inclusive  $\Delta\gamma$  measurement; the intercept is consistent with zero in Fig. 4 and finite with higher statistics data<sup>[27]</sup>. Similar analysis has recently been performed on 27 GeV data<sup>[28]</sup>. However, it has been found that residual flow-induced background remains because

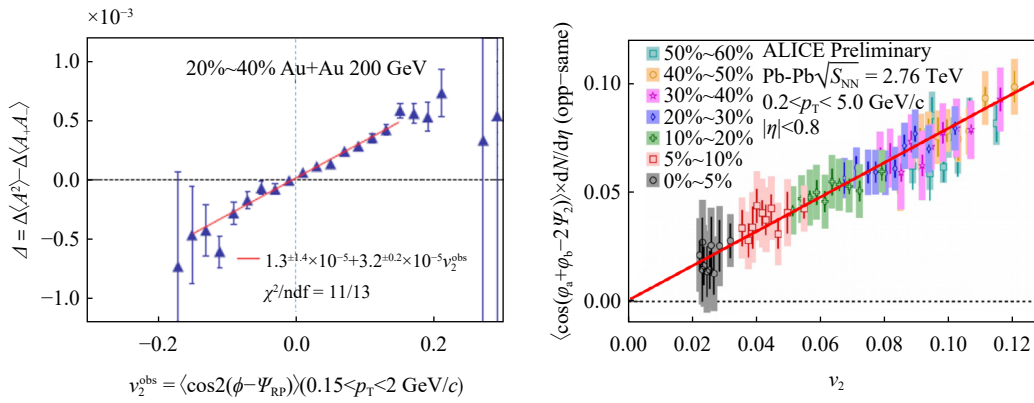


Fig. 5 (a) First attempt of event shape engineering (ESE) by RHIC/STAR<sup>[27]</sup> selecting events according to the elliptic anisotropy observable  $v_2^{\text{obs}} = \langle \cos 2(\phi_{\text{POI}} - \psi_{\text{EP}}) \rangle$  of the particles of interest (POI). The  $v_2^{\text{obs}}$  spreads over a wide range in value embracing zero, primarily because of statistical fluctuations. The coordinate quantity is a charge-dependent particle multiplicity asymmetry observable similar to  $\Delta\gamma$ . The intercept at  $v_2^{\text{obs}}=0$  is sensitive to CME with a large reduction of background contamination; however, the background is not completely eliminated because the resonance (correlation cluster) elliptic flow is not exactly zero when one forces  $v_2^{\text{obs}}=0$  of the final-state particles by primarily statistical fluctuations<sup>[29]</sup>. (b) ESE analysis by LHC/ALICE<sup>[30]</sup> selecting events in each narrow centrality bin according to the  $q_2$  elliptic flow vector in the forward and backward rapidity regions, exclusive from the POI's. The spread of the POI  $v_2$  on the abscissa is due only to dynamical fluctuations. The intercept of a “linear” fit in the multiplicity scaled  $\Delta\gamma$  versus  $v_2$ , sensitive to CME, is presently consistent with zero. The ESE analysis and results from CMS<sup>[31]</sup> are similar. (color online)

## 2.2 By varying signal

Isobar collisions were proposed<sup>[32]</sup> as an ideal means to cancel background: the same mass number of the  ${}^{96}_{44}\text{Ru}$  and  ${}^{96}_{40}\text{Zr}$  nuclei would ensure equal background, and the larger atomic number of the former would yield an approximately 15% stronger CME signal<sup>[33]</sup>. If the CME is 10% of the measured  $\Delta\gamma$ , then an isobar difference of 1.5% would be expected, representing a  $4\sigma$  effect with the data precision of 0.4% achieved in experiment<sup>[34–35]</sup>. However, because  $\Delta\gamma_{\text{Bkg}} \sim 1/N$  and the magnetic field is smaller in isobar collisions than in Au+Au, the signal to background ratio in the former may be significantly smaller<sup>[36]</sup>, which would result in a weaker significance.

Moreover, it has been shown by density functional theory (DFT) calculations that the isobar nuclear structures are not identical; although the charge radius of Ru is bigger, Zr possesses a significantly thicker neutron skin leading to

resonance/cluster  $v_2$ , primarily responsible for the CME background, does not vanish at the statistically engineered  $v_2^{\text{obs}}=0$ <sup>[29]</sup>.

The ALICE<sup>[30]</sup> and CMS<sup>[31]</sup> experiments have performed the ESE analysis by binning events according to the so-called  $q_2$  flow vector in the forward/backward regions and then studying  $\Delta\gamma$  as a function of the average  $v_2$  of POI in those events in each centrality bin<sup>[25]</sup>. The ALICE data are shown in Fig. 5 (right panel), where a linear relationship is observed. While analysis details differ, both ALICE and CMS found vanishing intercepts at  $v_2=0$ , suggesting a null CME signal. This method engineers on the dynamical fluctuations of  $v_2$ , and remains a promising means to extract the possible CME in future high statistics data.

its larger overall size<sup>[37–38]</sup>. This would yield larger  $N$  and  $v_2$  in Ru+Ru than Zr+Zr collisions at the same centrality<sup>[37, 39]</sup>. As a result, the backgrounds would be slightly different, with an uncertainty that may not be negligible, reducing the significance of isobar collisions<sup>[37]</sup>. Indeed, the isobar data show significant differences in  $N$  and  $v_2$  between the two systems<sup>[34]</sup>, consistent with DFT predictions<sup>[37, 39]</sup>.

Figure 6 shows the Ru+Ru/Zr+Zr ratio of various CME observables from STAR<sup>[34]</sup>. The ratio in  $\Delta\gamma/v_2$  being significantly below unity is due to the multiplicity ( $N$ ) difference. The more proper baseline would be the ratio in  $1/N$ , or unity for the ratio in  $N\Delta\gamma/v_2$ , the brown dashed line in Fig. 6. The  $\Delta\gamma$  data points are all above this line, which could imply that there may be finite CME signal in those isobar data<sup>[40]</sup>. However, the situation is more complicated because of nonflow effects<sup>[41–42]</sup> discussed in Sec. 3.

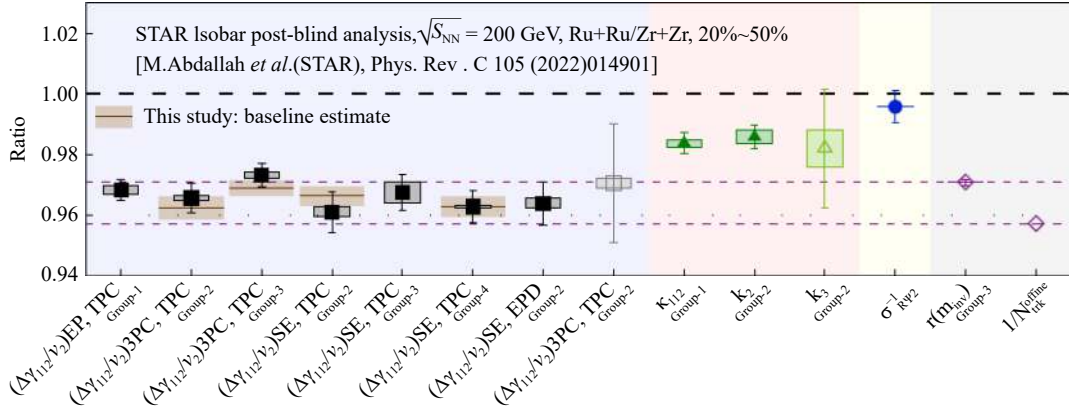


Fig. 6 The Ru+Ru/Zr+Zr ratios of the CME observable  $\Delta\gamma/v_2$  (black filled squares) from the isobar blind analysis by STAR<sup>[34, 42–43]</sup>. The ratios are below unity (the black dashed line), mainly because of the larger multiplicity dilution in Ru+Ru than in Zr+Zr. The multiplicity difference is caused by the slightly larger size of Zr than Ru arising from a thicker neutron skin in the Zr nucleus, a subtlety in nuclear structure predicted by the DFT calculations<sup>[37–38, 44]</sup>. If scaled by multiplicity (the right coordinate), the Ru+Ru/Zr+Zr ratios of  $N\Delta\gamma/v_2$  are above unity (the purple dashed line) and would indicate a finite CME signal<sup>[40]</sup> if the number of correlated background clusters is proportional to event multiplicity. However, the background cluster multiplicity is better represented by the relative excess of OS over SS pair multiplicity,  $r = (N_{OS} - N_{SS}) / N_{SS}$ <sup>[34]</sup>, the isobar ratio of which is indicated by the pink dashed line. The  $\Delta\gamma/v_2$  isobar ratio data points are below that line, suggesting negative CME signal if the only backgrounds are the flow-induced ones. Next-level background contaminations, from nonflow correlations in 3-particle correlator and in  $v_2$  measurements, are investigated and indicate that the background baselines of the Ru+Ru/Zr+Zr ratios of  $\Delta\gamma/v_2$  (shaded areas with uncertainties) are consistent with measurements<sup>[45–46]</sup>. An upper limit of 10% is extracted on the CME fraction at 95% confidence level<sup>[45–46]</sup>. (color online)

### 2.3 By varying both signal and background

A better comparative method than isobar collisions, called the SP/PP method, is to measure  $\Delta\gamma$  with respect to the spectator plane (SP) and the participant plane (PP) in the same event<sup>[47–48]</sup>. The PP and SP differ because of geometry fluctuations arising from the finite number of nucleons in nucleus<sup>[49]</sup>. Since the measurements are performed on the same event, the physics is guaranteed to be identical in the two measurements. The magnetic field, primarily produced by the spectator protons, is more closely connected to the SP; the anisotropic flow on the other hand, gener-

ated by interactions among the constituents in the collision zone, is more closely connected to the PP. The two  $\Delta\gamma$  measurements, therefore, contain different amounts of the CME signal and flow-induced background,  $\Delta\gamma = \Delta\gamma_{\text{Bkg}} + \Delta\gamma_{\text{CME}}$  (see sketches in Fig. 7). Their relative magnitudes are given by

$$\begin{aligned} \Delta\gamma_{\text{CME}}\{\text{PP}\}/\Delta\gamma_{\text{CME}}\{\text{SP}\} &= \Delta\gamma_{\text{Bkg}}\{\text{SP}\}/\Delta\gamma_{\text{Bkg}}\{\text{PP}\} \\ &= \langle \cos 2(\psi_{\text{PP}} - \psi_{\text{SP}}) \rangle \equiv a, \end{aligned} \quad (4)$$

where the  $a$  parameter, quantifying the opening angle between the SP and PP, can be measured by the final-state

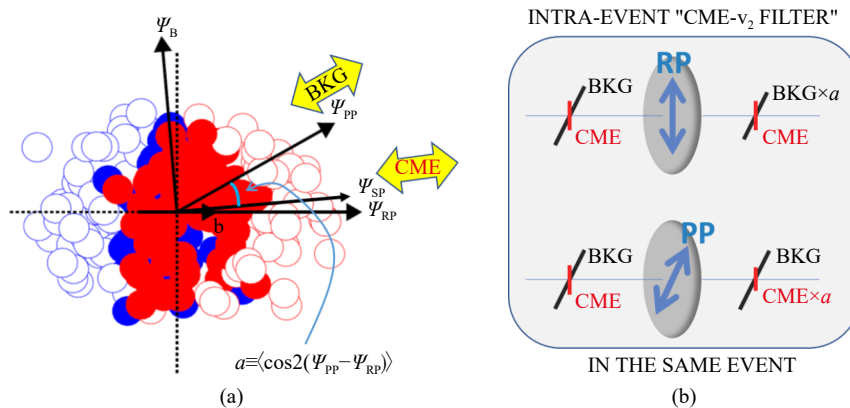


Fig. 7 Two  $\Delta\gamma$  correlators can be measured in the same collision event, one with respect to the participant plane (PP) and the other with respect to the spectator plane (SP, which is almost identical to the reaction plane RP as indicated by model calculations<sup>[47]</sup>). These two planes are not coincidental because of geometry fluctuations arising from finite number of nucleons in nucleus; the average opening angle between the two planes can be measured by final-state  $v_2$  with respect to the two planes,  $a \equiv \langle \cos 2(\psi_{\text{PP}} - \psi_{\text{SP}}) \rangle = v_2\{\text{SP}\}/v_2\{\text{PP}\}$ . The flow-induced background arises from elliptic flows of background sources and is the largest in  $\Delta\gamma$  with respect to PP and reduced by a factor  $a$  in that with respect to SP. The CME signal is related to the magnetic field and is the largest in  $\Delta\gamma$  with respect to RP and reduced by the same factor  $a$  in that with respect to PP. The SP and PP can be regarded as two filters for the CME signal and flow-induced background with respective transmission coefficients (as illustrated by the right sketch). (color online)

elliptic flow anisotropies with respect to the SP and PP,  $a = v_2\{\text{SP}\}/v_2\{\text{PP}\}$ . The  $\Delta\gamma$  measurements with respect to the SP and PP can therefore uniquely determine the CME signal and flow-induced background. One may in turn obtain the CME fraction as<sup>[47]</sup>

$$f_{\text{CME}} \equiv \frac{\Delta\gamma_{\text{CME}}\{\text{PP}\}}{\Delta\gamma\{\text{PP}\}} = \frac{A/a - 1}{1/a^2 - 1}, \quad (5)$$

where  $A \equiv \Delta\gamma\{\text{SP}\}/\Delta\gamma\{\text{PP}\}$ . Note that the magnetic field, because of event-by-event fluctuations, does not necessarily

point in the direction perpendicular to the SP<sup>[50]</sup>; however, the formalism is not affected<sup>[47]</sup> because what is quantified is the CME signal in the direction of the SP (and the PP).

Figure 8 shows the extracted  $f_{\text{CME}}$  and  $\Delta\gamma_{\text{CME}}$  in Au+Au collisions at  $\sqrt{s_{\text{NN}}} = 200$  GeV by STAR<sup>[51]</sup>. The peripheral data are consistent with zero CME with relatively large uncertainties. The mid-central 20%~50% data indicate a finite CME signal, with  $\sim 2\sigma$  significance.

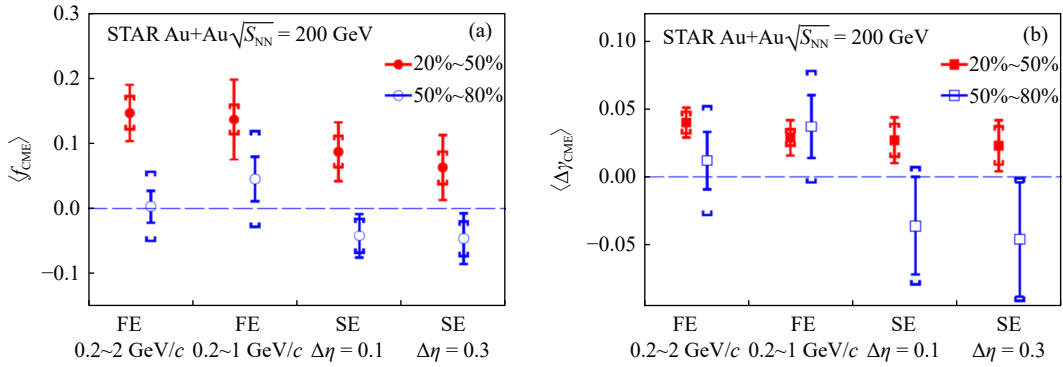


Fig. 8 The extracted CME fraction  $f_{\text{CME}}$  (a) and CME signal  $\Delta\gamma_{\text{CME}}$  (b) from  $\Delta\gamma$  measurements with respect to the SP and PP in Au+Au collisions at 200 GeV by STAR<sup>[47]</sup>. The four sets of data points are not independent but from the same 2.4 billion minimum-bias events using four analysis techniques/cuts: full-event (FE) where the POI's and the third particle  $c$  are from the entire STAR TPC acceptance within  $|\eta| < 1$  and with two  $p_T$  ranges,  $0.2 < p_T < 2$  GeV/c and  $0.2 < p_T < 1$  GeV/c, and sub-event (SE) where the POI's are from one side of the TPC acceptance and the third particle  $c$  is from the other side, and vice versa, with a small gap between the two sub-events,  $\Delta\eta = 0.1$  and  $\Delta\eta = 0.3$ , to suppress short-range correlations (such as HBT interference) and detector effects. While the peripheral data are consistent with zero CME, the midcentral data indicate a hint of positive CME with a significance of the order of  $2\sigma$ . The signal is on the order of 10% in terms of CME fraction in the inclusive  $\Delta\gamma$  measurement and on the order of a few  $\times 10^{-5}$  in terms of the absolute CME  $\Delta\gamma$  strength. (color online)

### 3 Next-level background: nonflow correlations

Experimentally, the EP used in the  $\gamma$  correlators is reconstructed by measured particles afforded by the very fact that particle azimuthal distributions are anisotropic. The EP resolution that quantifies the accuracy of the reconstructed EP and is used as a correction factor in measurements is calculated by EP correlations from different phase spaces<sup>[26]</sup>. Ideally one would want the EP to be the harmonic plane of pure flow, however, both the EP and the EP resolution are affected by the unavoidable nonflow correlations among particles. Nonflow correlations refer to all those correlations among particles that are unrelated to the global symmetry harmonic planes, such as correlations due to resonance decays, jets, and etc. The  $\gamma$  correlators are often calculated by the three-particle correlator,  $C_3 \equiv \langle \cos(\phi_\alpha + \phi_\beta - 2\phi_c) \rangle$ , divided by the  $v_2$  parameter of the third particle  $c$ ,  $\Delta\gamma = C_3 / v_2$ . The measured  $v_2$  is contaminated by nonflow, so it is propagated to the  $\gamma$  correlators<sup>[41–42]</sup>. The other nonflow contribution to  $C_3$  is simply from genuine 3-particle (3p) correlations.

The effects of nonflow on the isobar ratio can be ex-

pressed<sup>[42–43]</sup> as

$$\frac{(N\Delta\gamma/v_2^*)^{\text{Ru}}}{(N\Delta\gamma/v_2^*)^{\text{Zr}}} \approx \frac{\varepsilon_2^{\text{Ru}}}{\varepsilon_2^{\text{Zr}}} - \frac{\Delta\varepsilon_{\text{nf}}}{1 + \varepsilon_{\text{nf}}} + \frac{\varepsilon_3/\varepsilon_2}{Nv_2^2 + \varepsilon_3/\varepsilon_2} \left( \frac{\Delta\varepsilon_3}{\varepsilon_3} - \frac{\Delta\varepsilon_2}{\varepsilon_2} - \frac{\Delta N}{N} - \frac{\Delta v_2^2}{v_2^2} \right), \quad (6)$$

where  $N \approx N_r \approx N_z$  are POI multiplicities. The asterisk on  $v_2$  denotes it is nonflow contaminated, and  $\varepsilon_{\text{nf}} = (v_2^*/v_2)^2 - 1$ . Shorthand notations are  $\varepsilon_2 \equiv \frac{N_{2p}v_{2,2p}}{Nv_2} \langle \cos(\phi_\alpha + \phi_\beta - 2\phi_{2p}) \rangle$  and  $\varepsilon_3 \equiv \frac{N_{3p}}{2N} \langle \cos(\phi_\alpha + \phi_\beta - 2\phi_c) \rangle_{3p}$ .  $\Delta X = X^{\text{Ru}} - X^{\text{Zr}}$ , and variables without superscript refer to those in individual systems  $X \approx X^{\text{Ru}} \approx X^{\text{Zr}}$ . The first term in Eq. (6) r.h.s. characterizes deviation from  $N$  scaling—the background scales with  $N_{2p}/N^2$  rather than simply  $1/N$ . This implies that the baseline should be the ratio of  $r$ , the pink dashed line in Fig. 6<sup>[34]</sup>. The nonflow  $\varepsilon_{\text{nf}}$  can be assessed by  $(\Delta\eta, \Delta\phi)$  2p-correlation analysis. The 3p-correlation contribution can be estimated by HIJING (Heavy ion jet interaction generator<sup>[52]</sup>) which models jet-like correlations well. The advantage of using HIJING is that it does not contain anisotropic flow hence no flow-induced background so that 3p-correlations from HIJING are all nonflow. Preliminary results<sup>[42]</sup> indicate a good cancellation between the effect of  $v_2$

nonflow in the second term of Eq. (6) (positive, because  $\Delta\varepsilon_{\text{nr}} < 0$  due to the larger  $N$  in Ru+Ru) and the effect of 3p-correlations in the third term (negative); both are of the magnitude 0.5%~1%. The estimated baselines are indicated by the shaded bands in Fig. 6 where the band widths represent the total uncertainties<sup>[45–46]</sup>. It is found that the estimated baselines are consistent with experimental measurements. An upper limit on the CME fraction of 10% is extracted at the 95% confidence level<sup>[45–46]</sup>.

Similar to isobar collisions, the SP/PP method measures the ratio of two quantities as well, namely  $A/a = \frac{N\Delta\gamma(\text{SP})/v_2(\text{SP})}{N\Delta\gamma(\text{PP})/v_2(\text{PP})}$ . Simpler than the isobar data, only the PP measurements are contaminated by nonflow; the nonflow contribution is given by

$$A/a = (1 + \varepsilon_{\text{nr}}) \left/ \left( 1 + \frac{\varepsilon_3/\varepsilon_2}{Nv_2^2\{\text{PP}\}} \right) \right. \quad (7)$$

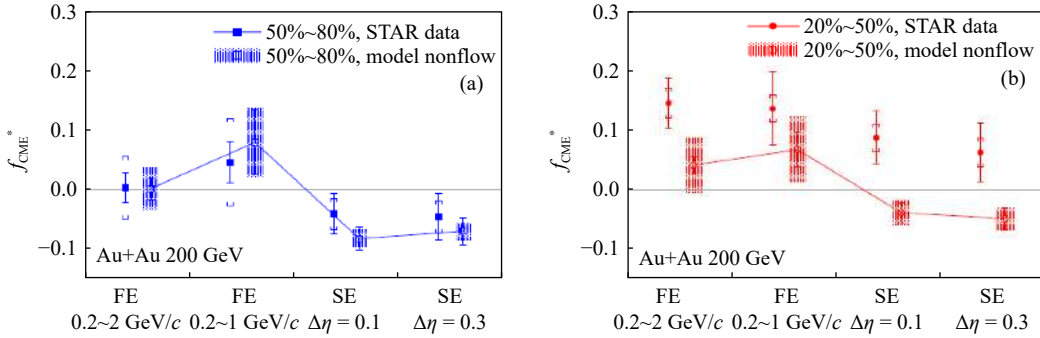


Fig. 9 The solid filled data points are the CME fractions extracted by the SP/PP method in peripheral (a) and midcentral (b) Au+Au collisions at 200 GeV<sup>[51]</sup>. These results are void of flow-induced backgrounds. The open points are the next-level background arising from 2-particle nonflow contamination in  $v_2$  measurements and 3-particle nonflow contamination in 3-particle correlator measurements<sup>[41]</sup>. The former is estimated by AMPT model (with string melting), and the latter is estimated by the HIJING model. The AMPT model is found to describe many aspects of experimental data well; the HIJING model is considered to model the 3-particle correlation well based on its agreement with data in peripheral collisions (non-peripheral collisions cannot be directly compared because of flow-induced background in data). The results indicate that the peripheral data are consistent with nonflow background estimation, and the midcentral data are generally above the estimated nonflow background, underscoring the intriguing prospect of a possible positive CME signal in the data. (color online)

## 4 Remarks

It has been an enduring journey in searching for the CME<sup>[18, 54–56]</sup>. A whole isobar run is devoted at RHIC<sup>[57]</sup>, accumulating over 4 billion MB events by the STAR detector<sup>[34]</sup>. Although only an upper limit can be extracted on the CME, it has provided many insights into the CME as well as a pleasant byproduct of probing nuclear structure and symmetry energy with relativistic collisions<sup>[37, 44]</sup>. Furthermore, the realization of a factor of several smaller CME signal expected in isobar than Au+Au collisions<sup>[36]</sup>, the non-observation of the CME in isobar collisions<sup>[34]</sup>, and the hint of 10% signal in Au+Au collisions<sup>[51]</sup> are all consistent and suggest that we are on the right track.

Meanwhile, many innovative methods have been invented. Two of the methods, the SP/PP method and the ESE method, are particularly promising. It is fair to say that

This nonflow contribution to  $A/a$  will yield a non-zero  $f_{\text{CME}}$  value. Nonflow in  $v_2$  yields a positive  $f_{\text{CME}}$  while 3p-correlations result in a negative  $f_{\text{CME}}$ . The former has been estimated by the AMPT (A Multi-Phase Transport<sup>[53]</sup>) model with string melting<sup>[41]</sup>. Work is on-going to extract this nonflow contribution from real data by  $(\Delta\eta, \Delta\phi)$  2p-correlations, as was done in isobar data aforementioned. The latter has been estimated by HIJING simulation of Au+Au collisions. There is a good degree of cancellation between the two, and the net effect could even be negative<sup>[41]</sup>. This is shown in Fig. 9 together with the  $f_{\text{CME}}$  measurements in Au+Au collisions<sup>[41]</sup>. Although model dependent, the results suggest that the measured positive  $f_{\text{CME}}$  in midcentral Au+Au collisions might indeed hint at a finite CME signal.

the flow-induced backgrounds have been well understood and are under control after extensive studies of many years. Further background effects due to nonflow correlations have been investigated, and can be reliably estimated for the SP/PP method and can be straightforwardly incorporated in future ESE analysis.

There appear two remaining issues. One is that the CME signal, originally oriented along the magnetic field direction, may tilt away further from the PP due to final-state particle rescattering effects<sup>[34, 58–59]</sup> because of a stronger signal reduction in the direction related to the PP (see Fig. 10). This would imply that the projection of CME onto the SP and PP directions are more complicated than the same factor  $a$  from final-state  $v_2$  measurements. As illustrated in Fig. 10, the final-state CME signal will project onto the PP through a larger opening angle, or a smaller factor  $b = \langle \cos 2(\psi_{\text{Fin,CME}} - \psi_{\text{PP}}) \rangle$  than the factor  $a$  [Eq. (4)];

the final-state CME signal will also have a projection factor onto the SP,  $b' = \langle \cos 2(\psi_{\text{Fin.CME}} - \psi_{\text{SP}}) \rangle$ . One thus obtains  $f_{\text{CME}} \equiv \frac{\Delta\gamma_{\text{CME}}^{\text{[PP]}}}{\Delta\gamma^{\text{[PP]}}} = \frac{A/a-1}{b'/(ab)-1}$ , instead of Eq. (5) (where, without final-state rescattering effects,  $b = a$  and  $b' = 1$ ). However, since  $b = ab'$ , the above  $f_{\text{CME}}$  expression reduces to Eq. (5). In other words, one does not need to know the factor  $b$  or  $b'$  to extract the CME fraction. This is analogous to the situation where the formulism is not affected by event-by-event fluctuations of the magnetic field direction<sup>[50, 47]</sup>, because the extracted  $f_{\text{CME}}$  is the fraction of the tilted CME measured with respect to the PP (and similarly the SP) out of the inclusive  $\Delta\gamma$  measurement.

The other issue is that there might be background contribution from vector meson spin alignment. An apparently large  $\phi$ -meson spin alignment has been observed<sup>[61]</sup>; it is conceivable that the spin alignment of the  $\rho$ -meson, which contributes significantly to the final-state pions, is also large. However, spin alignment is generated by spin-orbit interactions in the participant zone, and is therefore aligned with the PP. The spin alignment modifies the angular distribution of the decay daughters and thus their  $v_2$ . So the spin alignment contribution to  $\Delta\gamma$  is similar to and part of the flow-induced background, thus it is not an additional background but already taken care of in the SP/PP method.

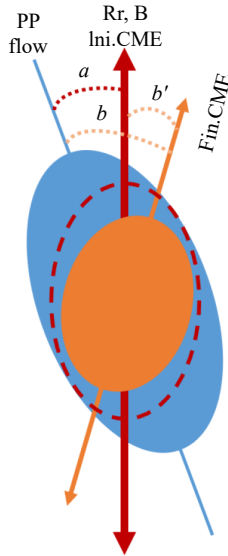


Fig. 10 Effects of final-state particle rescatterings on the CME signal. The initial CME signal is oriented along the magnetic field (illustrated by the dashed ellipse). Because of final-state interactions, the CME signal is reduced<sup>[59–60]</sup>, more so in the PP direction (note here for convenience the PP direction is drawn at  $90^\circ$  from the real PP) than in the direction perpendicular to it. This would result in a final-state CME signal (indicated by the solid yellow ellipse) that is oriented in a direction away further from the PP. The final-state CME signal measured with respect to PP and SP will both have a reduction factor,  $b$  and  $b'$ , respectively. However, since  $b = ab'$ , the  $f_{\text{CME}}$  formula of Eq. (5) remains, *i.e.*, one does not need to know  $b$  or  $b'$  to get the CME fraction. (color online)

## 5 Summary and outlook

In summary, the Chiral Magnetic Effect (CME) has been one of the most active and challenging fields of research in relativistic heavy-ion collisions. Measurements of the most commonly used  $\Delta\gamma$  observable are dominated by flow-induced backgrounds arising from particle correlations coupled with elliptic flow  $v_2$ . Many innovative methods have been invented to reduce or eliminate those backgrounds, including event shape engineering, isobar collisions, and measurements with respect to spectator and participant planes. While the first two yield a CME signal consistent with zero with the present statistics, the third indicates hint of a possible CME in Au+Au collisions at 200 GeV with  $2\sigma$  significance. After several years of extensive studies, the flow-induced backgrounds are now well understood and are under control.

All those methods are subject to further nonflow contaminations, the magnitudes of which are under active investigation. Preliminary results indicate that the isobar data can be understood by nonflow backgrounds, and the CME signal is consistent with zero. On the other hand, the hint of a possible positive CME signal in Au+Au collisions appears robust against nonflow contaminations.

To outlook, an order of magnitude increase in statistics is anticipated of Au+Au collisions from 2023 and 2025 by STAR. This, together with the increased detector acceptance and a new forward event-plane detector, would present a powerful data sample to either identify the CME or put a stringent upper limit on it.

## References:

- [1] AAD G, ABBOTT B, ABDALLAH J, et al. *Phys Rev Lett*, 2015, 114: 191803.
- [2] HATSUDA T, KUNIHIRO T. *Phys Rept*, 1994, 247: 221.
- [3] GRAHAM P W, IRASTORZA I G, LAMOREAUX S K, et al. *Ann Rev Nucl Part Sci*, 2015, 65: 485.
- [4] KHARZEEV D E, PISARSKI R D, TYTGAT M H G. *Phys Rev Lett*, 1998, 81: 512.
- [5] KHARZEEV D E, MCLERRAN L D, WARRINGA H J. *Nucl Phys A*, 2008, 803: 227.
- [6] FUKUSHIMA K, KHARZEEV D E, WARRINGA H J. *Phys Rev D*, 2008, 78: 074033.
- [7] ADAMS J, AGGARWAL M M, AHAMMED Z, et al (STAR). *Nucl Phys A*, 2005, 757: 102.
- [8] ADCOX K, ADLER S S, AFANASIEV S, et al (PHENIX). *Nucl Phys A*, 2005, 757: 184.
- [9] MCLERRAN L, SKOKOV V. *Nucl Phys A*, 2014, 929: 184.
- [10] VOLOSHIN S A. *Phys Rev C*, 2004, 70: 057901.
- [11] ABELEV B I, AGGARWAL M M, AHAMMED Z Z, et al (STAR). *Phys Rev Lett*, 2009, 103: 251601.
- [12] ABELEV B I, AGGARWAL M M, AHAMMED Z, et al (STAR). *Phys Rev C*, 2010, 81(2010): 054908.

- [13] ADAMCZYK L, ADKINS J K, AGAKISHIEV G, et al (STAR). *Phys Rev C*, 2013, 88: 064911.
- [14] ABELEV B, ADAM J, ADAMOVA D, et al (ALICE). *Phys Rev Lett*, 2013, 110: 012301.
- [15] WANG F Q. *Phys Rev C*, 2010, 81: 064902.
- [16] BZDAK A, KOCH V, LIAO J F. *Phys Rev C*, 2010, 81: 031901.
- [17] SCHLICHTING S, PRATT S. *Phys Rev C*, 2011, 83: 014913.
- [18] ZHAO J, WANG F. *Prog Part Nucl Phys*, 2019, 107: 200.
- [19] ACHARYA S, ADAMOVA D, ADLER A, et al (ALICE). *JHEP*, 2020, 9: 160.
- [20] KHACHATRYAN V, SIRUNYAN A M, TUMASYAN A, et al (CMS). *Phys Rev Lett*, 2017, 118: 122301.
- [21] ADAM J, ADAMCZYK L, ADAMS J R, et al (STAR). *Phys Lett B*, 2019, 798: 134975.
- [22] ABDALLAH M S, ADAM J, ADAMCZYK L, et al (STAR). *Phys Rev C*, 2022, 106: 034908.
- [23] CHOUDHURY S, DONG X, DRACHENBERG J, et al. *Chin Phys C*, 2022, 46: 014101.
- [24] ADAMCZYK L, ADKINS J K, AGAKISHIEV G, et al (STAR). *Phys Rev C*, 2014, 89: 044908.
- [25] SCHUKRAFT J, TIMMINS A, VOLOSHIN S A. *Phys Lett B*, 2013, 719: 394.
- [26] POSKANZER A M, VOLOSHIN S A. *Phys Rev C*, 1998, 58: 1671.
- [27] TU B. Poster at Quark Matter, 2015.
- [28] WEN F, WEN L, WANG G. *Chin Phys C*, 2018, 42: 014001.
- [29] WANG F, ZHAO J. *Phys Rev C*, 2017, 95: 051901.
- [30] ACHARYA S, ADAM J, ADAMOVA D, et al (ALICE). *Phys Lett B*, 2018, 777: 151.
- [31] SIRUNYAN A M, TUMASYAN T, ADAM W, et al (CMS). *Phys Rev C*, 2018, 97: 044912.
- [32] VOLOSHIN S A. *Phys Rev Lett*, 2010, 105: 172301.
- [33] DENG W T, HUANG X G, MA G L, et al. *Phys Rev C*, 2016, 94: 041901.
- [34] ABDALLAH M S, ABOONA B E, ADAM J, et al (STAR). *Phys Rev C*, 2022, 105: 014901.
- [35] SHI S, ZHANG H, HOU D, et al. *Phys Rev Lett*, 2020, 125: 242301.
- [36] FENG Y, LIN Y, ZHAO J, et al. *Phys Lett B*, 2021, 820: 136549.
- [37] XU H J, WANG X, LI H, et al. *Phys Rev Lett*, 2018, 121: 022301.
- [38] XU H J, LI H, WANG X, et al. *Phys Lett B*, 2021, 819: 136453.
- [39] LI H, XU H, ZHAO J, et al. *Phys Rev C*, 2018, 98: 054907.
- [40] KHARZEEV D E, LIAO J, SHI S. *Phys Rev C*, 2022, 106: L051903.
- [41] FENG Y, ZHAO J, LI H, et al. *Phys Rev C*, 2022, 105: 024913.
- [42] FENG Y. Poster at Quark Matter 2022.
- [43] WANG F. *Acta Phys Polon Supp*, 2023, 1: 15.
- [44] LI H, XU H, ZHOU Y, et al. *Phys Rev Lett*, 2020, 125: 222301.
- [45] STAR Collaboration, arXiv: 2308.16846.
- [46] STAR Collaboration, arXiv: 2310.13096.
- [47] XU H J, ZHAO J, WANG X, et al. *Chin Phys C*, 2018, 42: 084103.
- [48] VOLOSHIN S A. *Phys Rev C*, 2018, 98: 054911.
- [49] ALVER B, BACK B B, BAKER M D, et al (PHOBOS). *Phys Rev Lett*, 2007, 98: 242302.
- [50] BLOCZYNSKI J, HUANG X, ZHANG X, et al. *Phys Lett B*, 2013, 718: 1529.
- [51] ABDALLAH M, ADAM J, ADAMCZYK L, et al (STAR). *Phys Rev Lett*, 2022, 128: 092301.
- [52] WANG X N, GYULASSY M. *Phys Rev D*, 1991, 44: 3501.
- [53] LIN Z W, KO C M, LI B A, et al. *Phys Rev C*, 2005, 72: 064901.
- [54] KHARZEEV D E, LIAO J, VOLOSHIN S A, et al. *Prog Part Nucl Phys*, 2016, 88: 1.
- [55] LI W, WANG G. *Ann Rev Nucl Part Sci*, 2020, 70: 293.
- [56] KHARZEEV D E, LIAO J. *Nature Rev Phys*, 2021, 3: 55.
- [57] KOCH V, SCHLICHTING S, SKOKOV V, et al. *Chin Phys C*, 2017, 41: 072001.
- [58] SHI S, JIANG Y, LILLESKOV E, et al. *Ann Phys*, 2018, 394: 50.
- [59] CHEN B X, ZHAO X L, MA G L. arXiv, 2024, 2301: 12076.
- [60] MA G L, ZHANG B. *Phys Lett B*, 2011, 700: 39.
- [61] ABDALLAH M S, ABOONA B E, ADAM J, et al (STAR). *Nature*, 2023, 614: 244.

## 强相互作用中的对称性破缺—手征磁效应

王福强<sup>1)</sup>

(湖州师范学院理学院, 浙江 湖州 313000)

**摘要:** 手征磁效应 (CME) 指夸克—真空拓扑胶子场相互作用导致手征不平衡而引起沿强磁场方向的电荷分离。这种手征反常是量子色动力学 (QCD) 的基本性质, 因此对 CME 的观测将对我们理解 QCD 和大自然产生深远影响。在重离子碰撞中的对 CME 敏感的方位角关联  $\Delta\gamma$  的测量结果受到各向异性椭圆流引起的背景污染。现已通过几种新颖方法, 包括专门的同质异位素核碰撞运行项目, 来解决椭圆流引起的背景问题, 并研究了由非流关联引起的进一步背景效应。虽然同质异位素核碰撞结果与零 CME 信号一致 (上限为  $\Delta\gamma$  测量值的 10%), 但中间中心度 Au+Au 数据表明  $\Delta\gamma$  测量值中可能有 10% 的 CME 信号 (大概 2 个标准差的显著性)。未来增加的数据统计量以及改进的探测器功能应该会得出相对论重离子碰撞中 CME 存在或不存在的明确结论。

**关键词:** 手性磁效应; 电荷分离;  $\Delta\gamma$  关联; 椭圆流背景; 非流

收稿日期: 2023-08-09; 修改日期: 2024-01-10

基金项目: 国家自然科学基金资助项目 (12035006, 12075085); 科技部资助项目 (2020YFE020200)

1) E-mail: [fqwang@zjhu.edu.cn](mailto:fqwang@zjhu.edu.cn)